

above, in agreement with the model proposed. The electron concentration at the cathode is lower than for the opposite electrode¹⁸ when used as a cathode, indicating that for the results reported in this paper, $n_c > n_L$.

It is concluded that this crystal (doped with Ag and Al and having a bulk electron density of $8 \times 10^9 \text{ cm}^{-3}$ at low fields) with evaporated Au electrodes has a boundary electron density of $n_c = 8 \times 10^7 \text{ cm}^{-3}$, and shows a negative differential conductivity range with a slope steeper than -1 at about $E_{II} = 55 \text{ kV/cm}$. This value of n_c yields an effective work function $\psi_{\text{Au,CdS:Ag,Al}}$ ($505 \text{ m}\mu$, $10^{12} \text{ photon/cm}^2 \text{ sec}$) = 0.42 eV and was obtained for a temperature of -65°C and an optical excitation of $\sim 10^{12} \text{ photon/cm}^2 \text{ sec}$, with a band width of $10 \text{ m}\mu$ centered at $505 \text{ m}\mu$. The bulk electron density at high fields is decreased by more than two orders of magnitude, presumably by field quenching, and is about $2 \times 10^7 \text{ cm}^{-3}$ at $E_{III} \approx 205 \text{ kV/cm}$. The quasineutrality

¹⁸ The electrodes were evaporated at different runs; the electrode with lower n_c was less homogeneous and caused a less homogeneous cathode adjacent high-field domain.

curve $n_1(E)$ might¹⁹ have a form as given in Fig. 9. The experimentally obtained values are indicated by circles.

An experimental determination of a wider range of the $n_1(E)$ curve is currently under way, using as a virtual cathode with an easily variable boundary density a shadow region parallel to the cathode, and a variable low-intensity optical excitation in the shadow region. Results of these investigations are reported in Ref. 20.

ACKNOWLEDGMENTS

It is a pleasure to acknowledge very valuable discussions with G. A. Dussel and Dr. G. Doehler.

¹⁹ The Franz-Keldysh-effect band-edge shift tends to flatten the n_1 curve somewhat since the photoconductivity increases with increasing field due to increased absorption of the monochromatic optical excitation (for assumed homogeneous excitation in direction of the light beam). For very-high-field domains, inhomogeneous excitation in the direction of the light beam might influence the current and field distribution. These effects are neglected here.

²⁰ K. W. Boer, G. Doehler, G. A. Dussel, and P. Voss, Phys. Rev. **169**, 700 (1968).

Photoelectronic Properties of ZnSe Crystals*†

GERALD B. STRINGFELLOW‡ AND RICHARD H. BUBE

Department of Materials Science, Stanford University, Stanford, California

(Received 9 February 1968)

The photoelectronic properties of p -type ZnSe:Cu and of n -type self-activated ZnSe(SA) have been investigated in single crystals. Results for ZnSe:Cu may be described by a multivalent-copper-impurity model in which Cu^+ and Cu^{2+} ions substituting on the Zn sublattice are responsible for the red and green luminescence bands, respectively. The green luminescence emission (2.34 eV) is from the conduction band to the empty $\text{Cu}_{\text{Zn}}^{\times}$ center. One of the red emission bands (1.97 eV) is from the conduction band to the empty Cu_{Zn}' center; a second red band (1.95 eV) is from a shallow level near the conduction band to the empty Cu_{Zn}' center. The Cu_{Zn}' center is also the major sensitizing center for n -type photoconductivity in p -type ZnSe:Cu, and it is the dominant acceptor center controlling p -type conductivity. Optical absorption in the infrared is due to an internal transition within the $\text{Cu}_{\text{Zn}}^{\times}$, which has an (Ar) $3d^9$ electronic configuration, plus a transition from the valence band to the empty Cu_{Zn}' center. Several annealing and impurity-incorporation experiments performed on ZnSe:Cu support this model for the Cu luminescence centers. The sensitizing center for n -type photoconductivity in n -type ZnSe(SA) is not the same as that associated with Cu_{Zn}' in p -type ZnSe:Cu; it lies closer to the valence band and has a capture cross section for electrons 10^{-3} that of the Cu_{Zn}' sensitizing center.

INTRODUCTION

THE purpose of this investigation has been to examine the luminescence, photoconductivity, and optical absorption of single crystals of ZnSe:Cu and of self-activated ZnSe(SA), well characterized with

respect to impurities and structure. A major portion of the investigation has been devoted to p -type ZnSe:Cu crystals, but a number of measurements have been made for comparison on n -type ZnSe(SA).

Copper impurity has long played a central role in the photoelectronic properties of many II-VI compounds. Copper, substituting on the zinc sublattice in ZnSe is an acceptor. In the chemically neutral state, copper has an electronic structure of (Ar) $3d^{10}4s^1$; copper substituted for zinc, $\text{Cu}_{\text{Zn}}^{\times}$, therefore has the (Ar) $3d^9$ configuration. If the ionic approximation were perfectly valid and the $3d$ electrons were shielded from the valence and conduction band wave functions, the

* Supported in part by the U. S. Army Research Office (Durham), in part by the U. S. Army Engineers Research and Development Laboratories, Fort Belvoir, and in part by the Advanced Research Projects Agency through the Center for Materials Research at Stanford University.

† Based on a Ph.D. dissertation submitted by G. B. Stringfellow to Stanford University.

‡ Present address: Hewlett-Packard Laboratories, Palo Alto, Calif.

$3d^9$ orbitals would be split by the tetrahedral crystal field to give $3d(t)$ sixfold-degenerate and $3d(e)$ fourfold-degenerate levels. Evidence that electrons can be interchanged between the p orbitals of the valence band and the d orbitals of the transition-metal cobalt impurity in GaP has been provided by Loescher¹ and Baranowski *et al.*² in their finding that the absorption due to the cobalt $3d^7$ was removed by raising the Fermi level above the cobalt acceptor center. In ZnSe, which is more ionic than GaP, copper impurity might be expected to behave similarly.

Birman³ has recently done a linear combination of atomic orbitals calculation of the Cu_{Zn}^x level in closely related ZnS crystals. He concludes that there are two Cu_{Zn}^x levels in the forbidden gap of ZnS, the t levels with five electrons in six degenerate orbitals and the e levels with four completely filled orbitals. The t levels were found to be an admixture of states with 60% $Cu(3d(t))$, 35% $S(3s,3p)$, with 5% $Zn(4s,4p)$ states. The e state was 92% $Cu(3d(e))$. The results indicate that the Cu_{Zn}^x levels are near the valence band edge and that because of the $3d$, $3p$, and $4s$ admixture they are optically and electronically active levels, able to interchange electrons with conduction and valence band; this is particularly true of the $Cu(t)$ level. Evidence for such interchanges in terms of luminescence emission, excitation of luminescence and photoconductivity, optical absorption, quenching of photoconductivity, and quenching of luminescence is provided in the present investigation.

A summary of the conclusions about the nature of the multivalent copper impurity behavior in ZnSe:Cu crystals has previously been published,⁴ and details of the properties of a shallow level involved in several of the photoelectronic processes are described elsewhere.⁵ The principal contributions of the present work are the establishment that the luminescence emission transitions found in ZnSe:Cu occur either between the conduction band, or a level below the conduction band, and a hole captured by a Cu_{Zn}' center or by a Cu_{Zn}^x center; that the Cu_{Zn}' center is the dominant acceptor in p -type ZnSe:Cu and is also a sensitizing center for n -type photoconductivity; and that the electrical, optical, and photoconductivity properties of ZnSe:Cu can all be consistently described in terms of a multivalent copper impurity model involving a kind of self-compensation by the copper itself.

Comparison of the photoelectronic properties of p -type ZnSe:Cu with n -type ZnSe(SA) also contributes

to the long-standing question about the identity of sensitizing centers in II-VI compounds. The close similarity of photoelectronic phenomena involving sensitizing centers and those involving copper impurity^{6,7} has led Broser,⁸ for example, to propose that copper impurity is the sensitizing center in CdS, in spite of fairly detailed circumstantial evidence to the contrary.⁹ The present work shows that in p -type ZnSe:Cu a specific optical absorption, optical quenching, and excitation of hole photoconductivity are identifiable with transitions involving the $Cu_{Zn}^x d^9$ configuration; i.e., in p -type ZnSe:Cu, copper impurity is a sensitizing center for n -type photoconductivity. In n -type ZnSe(SA), however, the sensitizing center lies closer to the valence band than the copper impurity level, and has a capture cross section for free electrons only 10^{-3} times that of the copper sensitizing center. These results suggest that the sensitizing center in n -type (SA)-type II-VI compounds should be attributed to a defect-associated intrinsic imperfection.

EXPERIMENTAL

Materials

High-purity ZnSe was synthesized from 99.9999% Zn obtained from Cominco Electronic Materials and 99.999% Se obtained from the American Smelting and Refining Co. High-purity Spectrosil quartz was used at all stages of the operation, and diffusion of oxygen through the quartz at the growth temperatures was avoided by enclosing the evacuated quartz envelope in which the growth took place in a larger, thicker quartz tube which was itself evacuated to 10^{-6} Torr. Crystal growth was carried out by the closed tube vapor-growth technique at 1150–1250°C by moving the furnace past the capsule at 1 mm/h. Crystals of ZnSe obtained showed no detectable impurity in the emission spectrographic analysis, and showed only self-activated luminescence at liquid-nitrogen temperature. These crystals were used in experiments on n -type ZnSe(SA).

ZnSe:Cu crystals were grown in a similar manner with the addition of high-purity copper metal to produce the desired impurity concentrations. Most of the measurements were performed on crystals containing 30 ppm of Cu by emission spectrographic analysis. All of the copper appeared to be dissolved in the ZnSe. No precipitates could be seen in an optical microscope at 1000 \times magnification. Other crystals prepared with 100 ppm Cu did exhibit extensive precipitation. All of the ZnSe crystals grown were shown to be cubic by x-ray diffraction. Various post-growth experiments

¹ D. H. Loescher, J. W. Allen, and G. L. Pearson, J. Phys. Soc. Japan Suppl. 21, 239 (1962).

² J. M. Baranowski, J. W. Allen, and G. L. Pearson, Phys. Rev. 160, 627 (1967).

³ J. L. Birman, in Proceedings of the International Conference on Luminescence, Budapest, 1966 (unpublished).

⁴ G. B. Stringfellow and R. H. Bube, in *II-VI Semiconducting Compounds*, edited by D. G. Thomas (W. A. Benjamin, Inc., New York, 1967), p. 1315.

⁵ G. B. Stringfellow and R. H. Bube, J. Appl. Phys. (to be published).

⁶ R. H. Bube, J. Appl. Phys. 35, 586 (1964).

⁷ F. F. Morehead, J. Phys. Chem. Solids 24, 37 (1963).

⁸ I. Broser, in *Physics and Chemistry of II-VI Compounds*, edited by M. Aven and J. S. Prener (North-Holland Publishing Co., Amsterdam, 1967), p. 533.

⁹ R. H. Bube, in *Physics and Chemistry of II-VI Compounds*, edited by M. Aven and J. S. Prener (North-Holland Publishing Co., Amsterdam, 1967), p. 662.

involving annealing and impurity incorporation were carried out with the same procedural cautions used during crystal growth to avoid contamination.

Electrical contacts of In-Ga alloy were applied to *n*-type ZnSe crystals by etching the crystals in 20–30% Br in methyl alcohol, placing In-Ga beads on the surface, and heating in a dry hydrogen atmosphere at 300°C for 10 min. These contacts were shown to be Ohmic by potential probes on the crystal. Ohmic contacts for *p*-type crystals were much more difficult to achieve. The procedure finally adopted was to evaporate gold on the surface and then heat to 350°C in a dry-hydrogen atmosphere. These contacts were nearly Ohmic at room temperature, but became nearly blocking upon cooling to liquid-nitrogen temperature. Low-temperature photoconductivity even in the *p*-type ZnSe:Cu crystals was *n*-type, and therefore photoconductivity measurements could be made even at low temperatures with the In-Ga contacts.

Equipment

Measurements of photoconductivity and luminescence between 85 and 450°K were made using a specially constructed Dewar similar to that described by MacDonald and Bube,¹⁰ utilizing a helium atmosphere for temperature control of the sample. Measurements of luminescence and optical absorption down to 16°K were performed in a Linde Dewar.

Various instruments were used in different phases of the work. (a) Luminescence emission spectra were obtained by using a Jarrel Ash Ebert monochromator with a resolution of 16.5 Å, RCA 1P21 or RCA 7102 cooled photomultiplier tubes, and photoexcitation by a focused 500-W Osram HBO mercury arc lamp. (b) Excitation spectra were obtained by excitation with a 45-W quartz-iodine lamp focused on the slit of a Bausch and Lomb monochromator. (c) Optical quenching spectra for photoconductivity and luminescence were determined at 85°K by exciting the crystal with light from a tungsten lamp passed through two 4660 Å interference filters; quenching radiation was supplied by the Bausch and Lomb monochromator. (d) Hall-effect and electrical-conductivity measurements were made in an Andonian liquid-helium Dewar, using Cary 31 CV vibrating reed electrometers as voltage detectors. (e) Optical-absorption measurements were made on a Cary 14 recording spectrophotometer between 0.4 and 2.5 μ, and on a Perkin-Elmer 621 infrared spectrophotometer between 2.5 and 50 μ.

RESULTS FOR ZnSe:Cu

Hall Effect and Conductivity

Hall-effect and electrical-conductivity measurements were made on the ZnSe:Cu crystals in the dark to

¹⁰ H. E. MacDonald and R. H. Bube, Rev. Sci. Instr. 33, 53 (1962).

determine conductivity type, location of Fermi level, carrier mobility, and ionization energy of Cu acceptors. The dark conductivity ($10^{-10} \Omega^{-1} \text{cm}^{-1}$) is due to holes with a mobility of approximately 30 $\text{cm}^2/\text{V sec}$ at 296°K. The Fermi level at 296°K is located 0.69 eV above the valence band. From the temperature dependence of hole density between 300 and 450°K, an activation energy of 0.72 eV for the Cu acceptors is determined, and the experimental data over this limited range are consistent with $3 \times 10^{17} \text{cm}^{-3}$ acceptors (assumed from spectrographic determination of Cu concentration) and 10^{17}cm^{-3} donors.

Photoconductivity and Photo-Hall Effects

The variation of photocurrent and photo-Hall mobility with temperature between 7 and 350°K is shown in Fig. 1. Below 300°K the photoconductivity is *n* type; this *n*-type photoconductivity is thermally quenched near 300°K, and the Hall mobility reverts to *p* type. The results are quite similar to those found in GaAs:Cu.¹¹ The reduction in photocurrent below 70°K is a genuine lifetime effect and is associated with the effects of shallow levels lying 0.012 eV below the conduction band.⁵ The photoconductivity lifetime at 85°K is about 3 μsec.

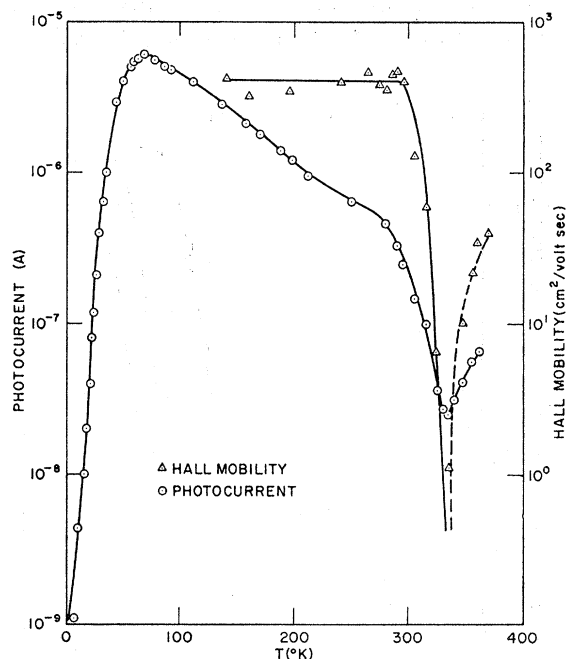


Fig. 1. Photocurrent and photo-Hall mobility as a function of temperature for ZnSe:Cu. The solid mobility curve represents *n*-type conductivity, the dashed curve *p*-type conductivity.

¹¹ R. H. Bube and H. E. MacDonald, Phys. Rev. 128, 2071 (1962).

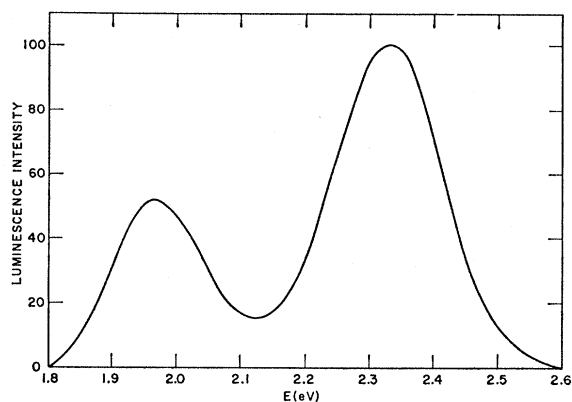


FIG. 2. Typical luminescence emission spectrum for ZnSe:Cu at 77°K, showing the red (1.97 eV) and green (2.34 eV) bands.

Luminescence Emission

A typical luminescence emission spectrum at 77°K is shown in Fig. 2. A red emission band has a maximum at 1.97 eV and a half-width of 0.18 eV. A green band, the more intense of the two, has a maximum at 2.34 eV and a half-width of 0.20 eV. No other emission was found between 1 and 2.8 eV. If the spectrum is measured at 16°K, a red band is found with a maximum at 1.95 eV that is over an order of magnitude more intense than the 1.97 eV band at 77°K. It is this low-temperature 1.95 eV emission which has been associated with a pair transition involving the 0.012-eV shallow levels.⁵

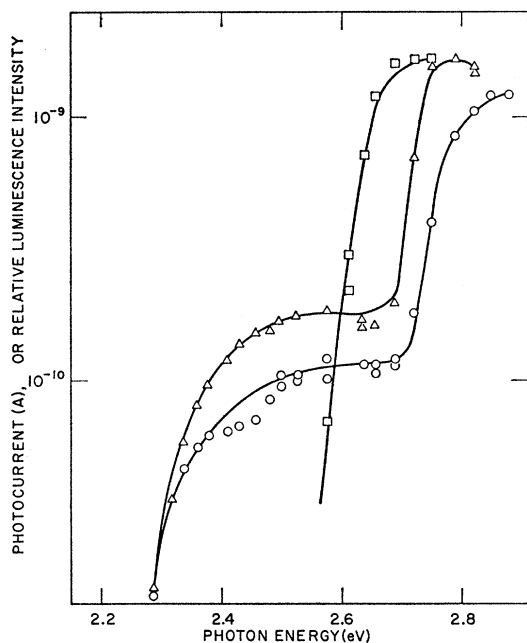


FIG. 3. Excitation spectra for photoconductivity and luminescence in ZnSe:Cu at 85°K. Curves are Δ photoconductivity, \circ red luminescence, and \square green luminescence.

The location of the maximum of the green band was found to increase linearly with temperature between 80°K (2.33 eV) and 220°K (2.25 eV) with a rate of 5.9×10^{-4} eV/°K, which may be compared to 7.1×10^{-4} eV/°K for the band gap.

Excitation of Photoconductivity and Luminescence

Excitation spectra of photoconductivity and both luminescence bands were measured at 85°K to determine whether the excitation of the luminescence bands results in photoconductivity. Simultaneous photo-Hall measurements were made to determine the sign of the carriers excited.

The excitation spectra shown in Fig. 3 indicate that two intrinsic transitions are involved in addition to the intrinsic band-gap excitation. One of these transitions has a low-energy threshold of 2.3 eV and excites red luminescence and photoconductivity. The other transi-

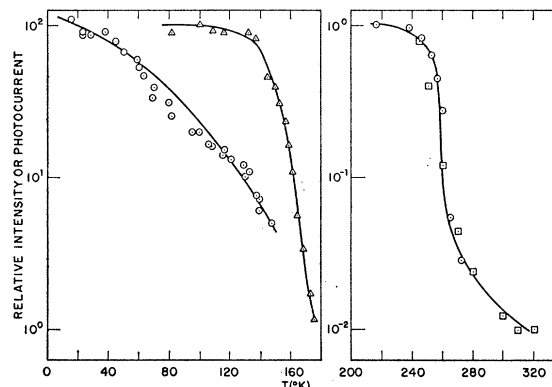


FIG. 4. Luminescence intensity and photocurrent versus temperature in ZnSe:Cu from 16 to 320°K. Curves are \circ 1.95-eV red luminescence between 16 and 140°K and 1.97-eV red luminescence between 216 and 320°K, Δ green luminescence, and \square photocurrent.

tion has a low-energy threshold of 2.6 eV and excites green luminescence; because of excitation of photoconductivity by the first transition, no specific information can be obtained about excitation of photoconductivity by the 2.6 eV transition. The photoconductivity excited in the extrinsic range for 2 to 3 eV was *n* type, however, and the Hall mobility was constant, independent of the wavelength of the exciting radiation.

Thermal Quenching of Photoconductivity and Luminescence

The temperature dependence of photocurrent and luminescence emission intensity is shown in Fig. 4 between 16 and 320°K. The 1.95-eV band associated with a pair transition⁵ quenches first near 50°K with an activation energy of 0.012 eV. The 2.34-eV green emission quenches at 140°K with an activation energy of 0.35 eV. Finally the 1.97-eV red band and the

photoconductivity quench simultaneously at 250°K with an activation energy of about 0.8 eV.

Optical Quenching of Photoconductivity and Luminescence

The optical quenching spectra for photoconductivity at 85°K and at 296°K are given in Fig. 5. The quenching spectrum has a low-energy threshold at about 0.7 eV, with some evidence for quenching at lower energies at 85°K. The low-energy threshold of the quenching below 0.5 eV could not be determined because of lack of high-intensity monochromatic excitation in this spectral region. The absence of the low-energy quenching tail at 296°K is not surprising,

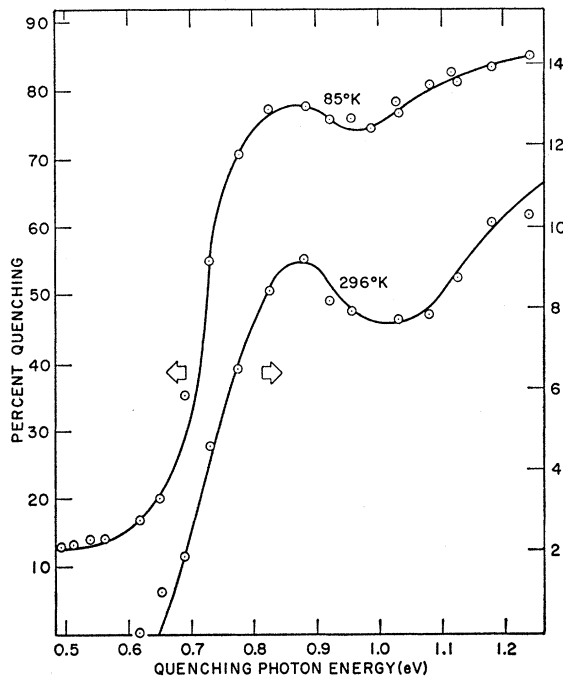


FIG. 5. Optical quenching spectra for photoconductivity in ZnSe:Cu at 85 and 296°K. Note that the 85°K curve should be read by the left scale, and the 296°K curve by the right scale.

since a level closer than 0.5 eV to the valence band would be thermally emptied at 296°K.

Figure 6 compares the quenching spectra for both luminescence bands with that for photoconductivity. Quenching for photoconductivity and the 1.97-eV red band are similar. Quenching for the green band is appreciably less above 0.7 eV and appreciably greater below 0.7 eV.

When crystals were excited at 85°K with 2.5 eV radiation such that the red but not the green emission was excited, optical quenching of the red emission caused a transient stimulation of the green emission. The spectra for the quenching of the red and stimulation of the green are identical. Typical curves are shown in

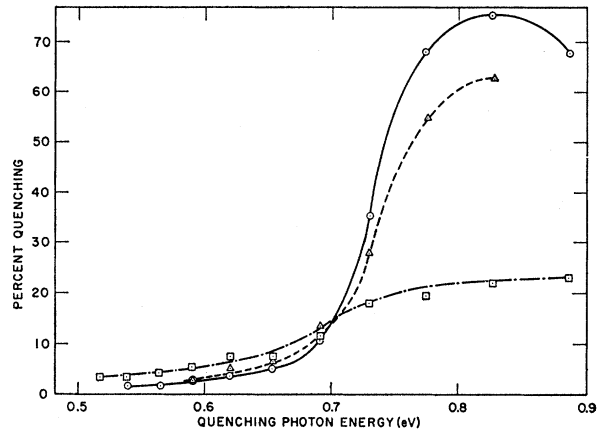


FIG. 6. Optical quenching spectra for photoconductivity and luminescence at 85°K. Curves are \odot photoconductivity, Δ red luminescence, and \square green luminescence.

Fig. 7. This effect can be interpreted as capture of holes by green centers after these holes are freed from red centers by optical quenching, followed by recombination of free electrons at green centers. Note that the lower-than-0.7-eV tail is absent from the red quenching spectrum in Fig. 7 for extrinsic excitation as compared to Fig. 6 for intrinsic excitation. This is because the lower energy levels are not active in recombination until holes are released from the 0.7-eV levels.

An attempt was made to determine the electron capture cross sections of the sensitizing centers for photoconductivity by determining the conditions for

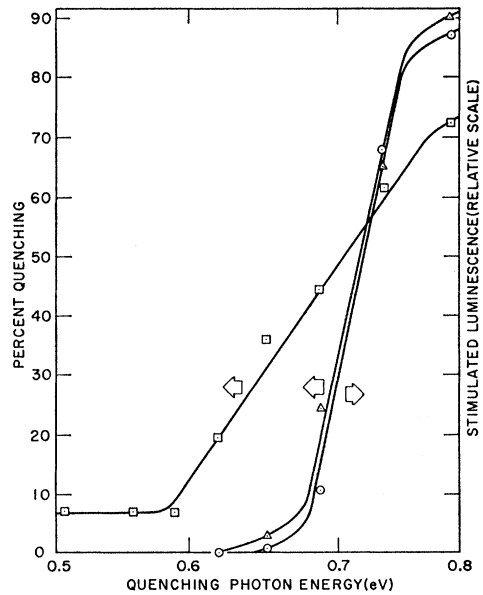


FIG. 7. Optical quenching of red luminescence and simultaneous stimulation of green luminescence at 85°K. Curves are \square quenching of the green emission, \odot quenching of red emission, and Δ maximum transient stimulation of green emission.

TABLE I. Determination of electron capture cross sections from onset of optical quenching.

	Quenching intensity (photons/cm ² sec)	Free electron density at onset of quenching (cm ⁻³)	Capture cross section of sensitizing center (cm ²) ^a
ZnSe: Cu	4.2×10^{13}	8×10^7	3.2×10^{-19}
Quenching by 0.77-eV photons	1.3×10^{14}	2.7×10^8	2.9×10^{-19}
	7.2×10^{14}	1.3×10^9	3.3×10^{-19}
	5.5×10^{15}	6.7×10^9	4.9×10^{-19}
ZnSe: Cu	6.2×10^{14}	6.1×10^8	8.2×10^{-19}
Quenching by 0.54-eV photons			
ZnSe (SA)	6.5×10^{14}	5.2×10^{11}	2.8×10^{-22}
Quenching by 0.88-eV photons	2×10^{16}	1.5×10^{12}	2.9×10^{-22}
	6×10^{15}	4.7×10^{12}	2.9×10^{-22}
	2.5×10^{16}	1.7×10^{13}	3.4×10^{-22}
	10^{17}	4.9×10^{13}	4.5×10^{-22}

^a Assuming a cross section for optical absorption of quenching radiation of 10^{-17} cm².

the onset of optical quenching.¹² Results obtained at 85°K are summarized in Table I. A value of 4×10^{-19} cm² is determined from measurements of quenching at 0.77 eV, and a less reliable value of 8×10^{-19} cm² is determined from measurements of quenching at 0.54 eV.

Infrared Absorption

Optical density as a function of wavelength was measured for the ZnSe:Cu crystals. The absorption coefficient was calculated from the results by correcting for reflection using the reflectivity data of Marple.¹³

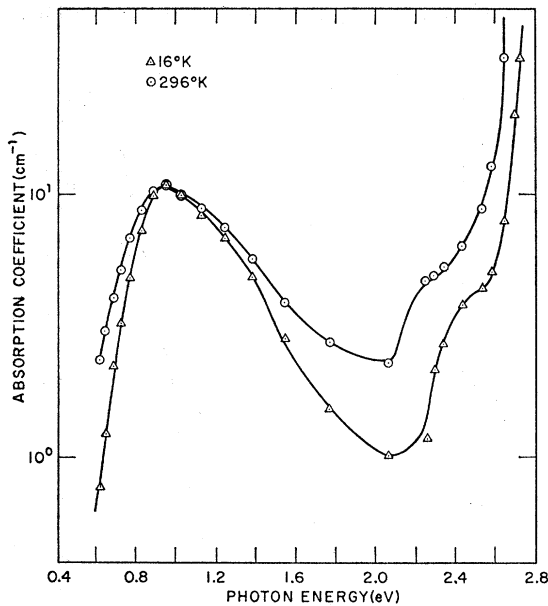


FIG. 8. Absorption coefficient as a function of photon energy for ZnSe:Cu at 16 and 296°K.

¹² R. H. Bube and F. Cardon, J. Appl. Phys. 35, 2712 (1964).

¹³ D. T. F. Marple, General Electric Research Rept. No. 63-RL-3466G, 1963 (unpublished).

The absorption coefficient shows a broad peak in the infrared at 0.93 eV and a subsidiary edge at 2.3 eV, in addition to the band gap at 2.7 eV, as shown in Fig. 8. Absorption measurements carried out to 5μ showed no additional structure.

An attempt was made to determine if photoconductivity is produced by the transition responsible for the 0.93 eV absorption. From photo-Hall effect and conductivity measurements it was found that the transition excites *p*-type photoconductivity, although the excitation and absorption spectra are different on the high-energy side of the maximum, as shown in Fig. 9. The excitation spectrum for *p*-type photoconductivity is seen to be identical with the optical quenching spectrum for *n*-type photoconductivity (Fig. 5), and appears to be composed of a band superposed on a flat

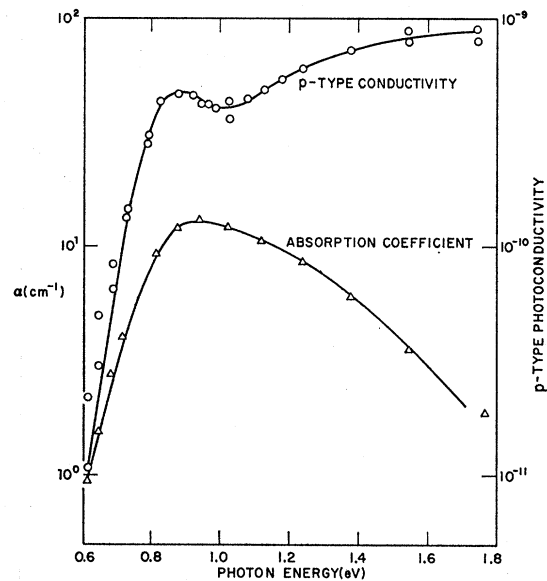


FIG. 9. Excitation spectrum for *p*-type photoconductivity and optical absorption in the infrared in ZnSe:Cu at 296°K.

response terminating in a low-energy threshold. It thus appears that two different types of transitions are involved in each of the following phenomena: absorption, excitation of *p*-type photoconductivity, and quenching of *n*-type photoconductivity.

RESULTS FOR ZnSe(SA)

Dark Conductivity and Hall Effect

The dark conductivity of self-activated ZnSe was too low to be measured even at temperatures of 450°K. A conductivity of 10^{-12} (Ω cm)⁻¹ was the limit of the apparatus; thus the dark Fermi level is at least 1.25 eV from either band, and hence near the center of the gap. This is typical of a well-compensated material.

Photoconductivity and Photo-Hall Effect

Photoconductivity and photo-Hall effect were measured between 77 and 296°K. The results are given in Fig. 10. The electron mobility is a factor of two higher in ZnSe(SA) than in ZnSe:Cu. Thermal quenching of photoconductivity occurs near 300°K with an activation energy of 0.60 eV. The photoconductivity lifetime is 610 μ sec at 85°K, quenching to 0.6 μ sec at 350°K.

Luminescence Emission

The luminescence emission spectrum at 85°K for ZnSe(SA) is given in Fig. 11. The emission consists of

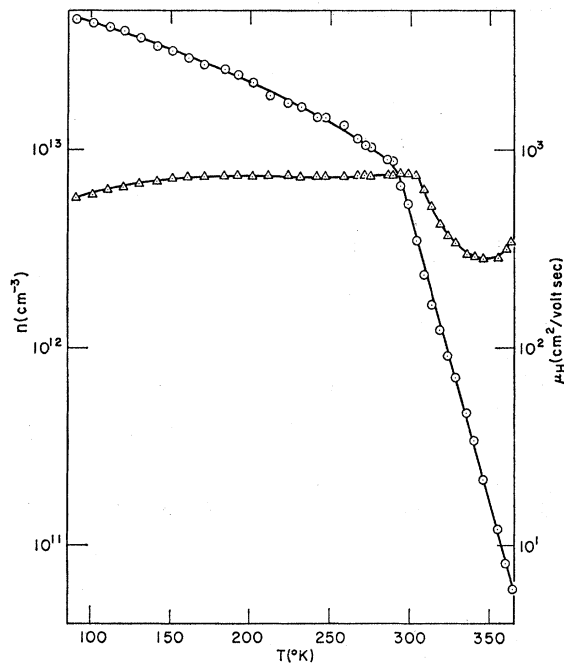


FIG. 10. Photoexcited electron density and photo-Hall mobility as a function of temperature in ZnSe(SA). Curves are \odot electron density and \triangle Hall mobility.

a broad band with maximum at 2.03 eV and 0.315-eV half-width. The fact that the shape of this emission band changes with temperature suggests that several sub-bands may be involved.

Excitation of Photoconductivity and Luminescence

Excitation spectra at 85°K for luminescence and photoconductivity in ZnSe(SA) are given in Fig. 12. The spectra are quite complex; indications of transitions from levels lying about 1.9, 2.2, and 2.6 eV from the conduction band are found, all of which yield n -type photoconductivity, and at least the two higher energy transitions also excite luminescence.

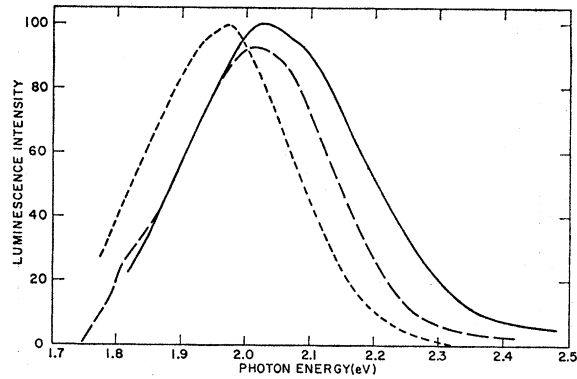


FIG. 11. Luminescence emission spectra at 85°K for ZnSe(SA) (solid curve), ZnSe:Cu annealed in Zn (large-dash curve), and ZnSe:Cu with diffused Al (small-dash curve).

Optical Quenching of Photoconductivity and Luminescence

The optical quenching spectra for photoconductivity and luminescence at 85°K are shown in Fig. 13. The spectrum has a very broad low-energy threshold beginning at about 0.5 eV. The data could be interpreted as exhibiting a threshold at about 0.6 eV for a quenching process more effective for luminescence than for photoconductivity, with a second threshold at 0.5 eV for the photoconductivity. Comparison with Fig. 6 for the quenching spectra for ZnSe:Cu indicates that the

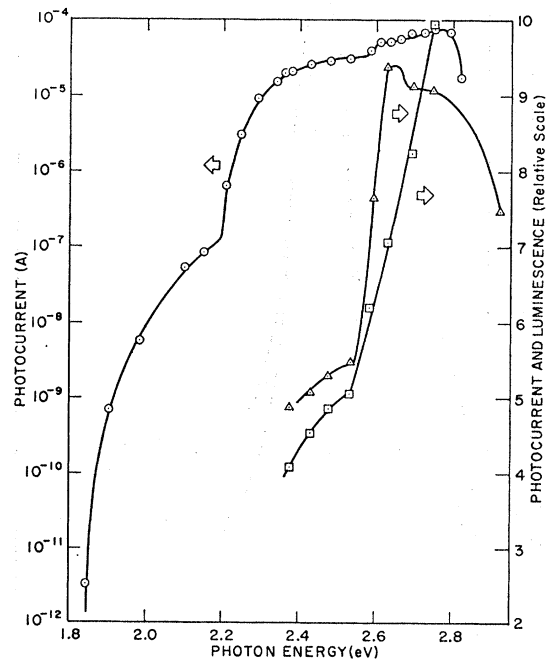


FIG. 12. Excitation spectra for luminescence and photoconductivity at 85°K in ZnSe(SA). Curves are \odot , \square photocurrent, and \triangle luminescence. Note that the left photocurrent curve should be read on the left log scale, and that the two right curves should be read on the right linear scale.

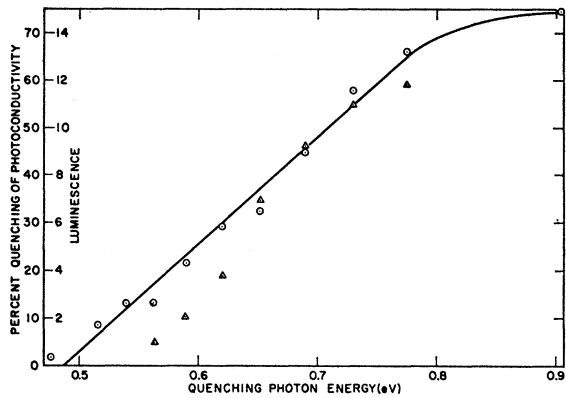


FIG. 13. Optical quenching spectra for photoconductivity and luminescence in ZnSe(SA) at 85°K. Curves are \odot photoconductivity, and \triangle luminescence.

levels involved in ZnSe(SA) are closer to the valence band than those in ZnSe:Cu.

The capture cross section of the sensitizing centers in ZnSe(SA) was determined at 0.88 eV by the onset of quenching method.¹² The results, given in Table I, indicate a cross section of 3×10^{-22} cm², some three orders of magnitude smaller than that associated with sensitizing centers in ZnSe:Cu crystals. The difference in lifetime between the two types of crystal is consistent with this cross-section difference.

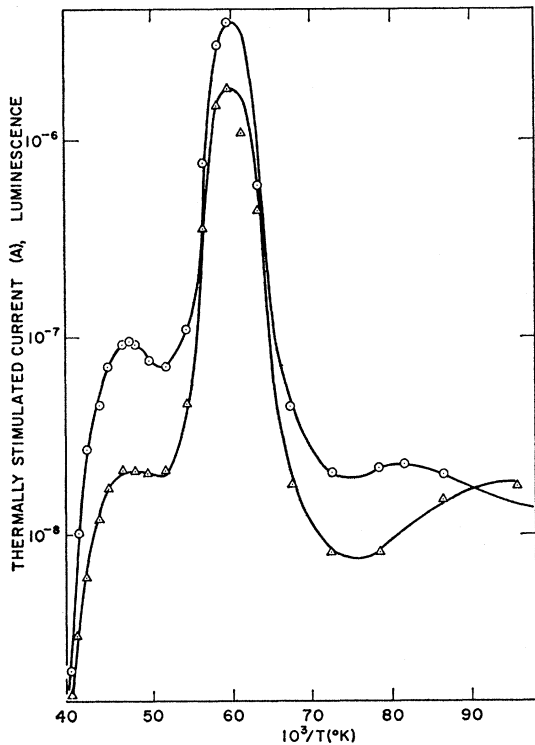


FIG. 14. Thermally stimulated current and luminescence in ZnSe(SA). Curves are \odot current, and \triangle luminescence.

Thermally Stimulated Conductivity and Luminescence

The ZnSe(SA) crystals contain many deep electron traps. Large thermally stimulated conductivity (TSC) and thermally stimulated luminescence (TSL) peaks were found, as shown in Fig. 14. The TSC values were large enough that it was possible to make thermally stimulated Hall-effect measurements; results are given in Fig. 15. The trap depths of the two deeper traps were determined by the method of decayed TSC¹⁴ to be 0.28 and 0.38 eV; the density of the 0.28 eV trap was estimated to be 10^{16} cm⁻³.

Optical Absorption

The optical absorption coefficient in ZnSe(SA) was calculated from the optical density in the same way

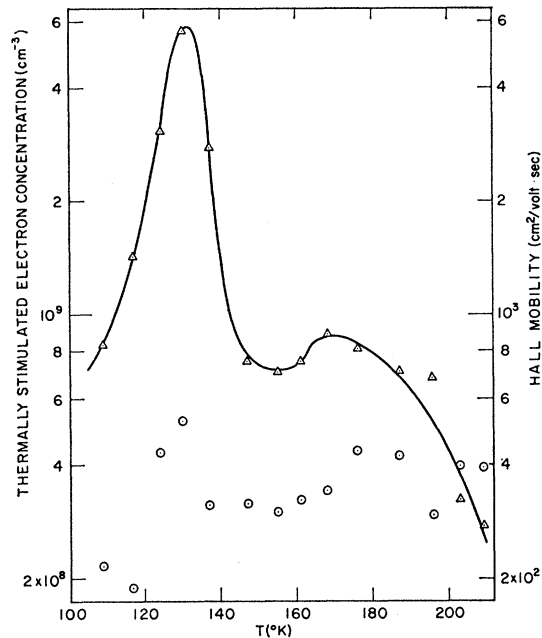


FIG. 15. Hall mobility and electron concentration measured during a thermally stimulated current experiment. Curves are \odot Hall mobility, and \triangle electron concentration.

described previously for ZnSe:Cu. At room temperature two thresholds at about 2.2 and 2.6 eV were found, corresponding to the excitation thresholds.

ANNEALING AND IMPURITY INCORPORATION

In order to provide additional data by which to judge the validity of a model developed for luminescence and photoconductivity in ZnSe:Cu and ZnSe(SA) crystals, several experiments were done involving annealing in Zn or Se vapor, or involving incorporation of impurities such as Al, in addition to Cu.

¹⁴ G. A. Dussel and R. H. Bube, Phys. Rev. 155, 764 (1967).

TABLE II. Summary of properties of ZnSe containing various impurities and annealed in various ways.

Sample	Green		Red		I_G/I_R	$E_F(300^\circ\text{K})$ (eV)	$\tau(85^\circ\text{K})$ (μsec)
	E_{max} (eV)	$E_{1/2}$ (eV)	E_{max} (eV)	$E_{1/2}$ (eV)			
ZnSe (as grown)			2.03	0.315			613
ZnSe:Cu (as grown)	2.35	0.20	1.96	0.18	1.9	0.69 (p)	3
ZnSe:Cu (Se annealed)	2.34	0.23	1.96	0.14	7.0	0.58 (p)	0.3
ZnSe:Cu:Al (as grown)			1.94	0.18	0.04	0.82 (n)	29
ZnSe:Cu:Al (diffused)			1.98	0.27			
ZnSe:Cu (Zn annealed)			2.02	0.28			

Annealing and Impurity Incorporation Procedures

Se Annealing

A crystal of ZnSe:Cu was annealed at 1000°C for 24 hours in Se vapor at a pressure of 1 atm. Annealing increased the p -type conductivity, and increased the ratio of green to red luminescence intensity.

Zn Annealing

Several ZnSe:Cu crystals were annealed in liquid Zn at 900°C for 24 h. These crystals exhibited self-activated luminescence after annealing, as shown in Fig. 11.

Al Incorporation

An attempt was made to incorporate Al donors into ZnSe:Cu by diffusion after evaporation of Al onto the crystals. Aven and Halsted¹⁵ found that Al diffuses very slowly in ZnSe:Cl, probably because of association between the charged Al donors and negatively charged intrinsic acceptors. The diffusion would be expected to be slow in ZnSe:Cu because of the high density of foreign acceptors with which Al can associate. It was found necessary to diffuse Al at 900°C for 12 h to incorporate the Al into the ZnSe:Cu. The resulting crystals were highly conducting and the luminescence was a combination of the copper-red and the self-activated luminescence.

Al was incorporated most successfully by adding Al and Cu during the growth of the ZnSe. The result was ZnSe with 40-ppm Cu and 40-ppm Al.

Measurement of Annealed ZnSe Crystals

Table II summarizes the position of the Fermi level, electron lifetime, and luminescence properties of the ZnSe crystals with various impurities, and annealed in several ways.

The infrared absorption band present in ZnSe:Cu crystals was removed by incorporating Al or other donors, or by annealing in Zn.

Figure 16 shows the emission spectra for ZnSe:Cu, ZnSe:Cu:Al, and Se-annealed ZnSe:Cu crystals. Annealing in Se increases the green-to-red intensity ratio, and incorporation of Al decreases the ratio. Figure 11 compares the emission spectra of ZnSe(SA), Zn-

annealed ZnSe:Cu, and ZnSe:Cu:Al after diffusion of Al into the crystal. Apparently the Zn annealing removed Cu from the crystal by solvent extraction,¹⁶ producing self-activated luminescence. Zn vacancies are produced to compensate the Al donors incorporated during the Al diffusion, thus forming ($V_{\text{Zn}}\text{Al}_{\text{Zn}}$) self-activated luminescence centers. The density of these centers becomes so large that the self-activated luminescence dominates the Cu luminescence.

It was possible to observe simultaneous TSC and TSL in the ZnSe:Cu:Al crystals. Figure 17 shows that both luminescence bands have the same TSL maximum as the TSC maximum. Experimental limitations prevented accurate measurement of TSL in the side peaks. The trap depths found here are identical with those found in ZnSe(SA) and shown in Fig. 14.

DISCUSSION

Physical Model for Red and Green Luminescence in ZnSe:Cu

To facilitate discussion of the results, an energy-level model is proposed which consistently describes the results as set forth in the previous sections. This model is given in Fig. 18, where the following transitions are indicated. E_B is the energy band gap of 2.7 eV. T are shallow traps lying 0.012 eV below the conduction band.⁵ E_R is the excitation of red luminescence and electron photoconductivity with a value of 2.3 eV. I_{R1}

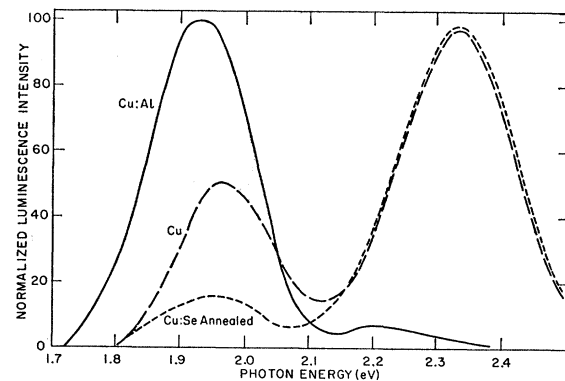


Fig. 16. Luminescence emission spectra at 85°K for ZnSe:Cu:Al, ZnSe:Cu as grown, and ZnSe:Cu annealed in Se.

¹⁵ M. Aven and R. E. Halsted, Phys. Rev. 137, A228 (1965).

¹⁶ M. Aven and H. H. Woodbury, Appl. Phys. Letters 1, 53 (1962).

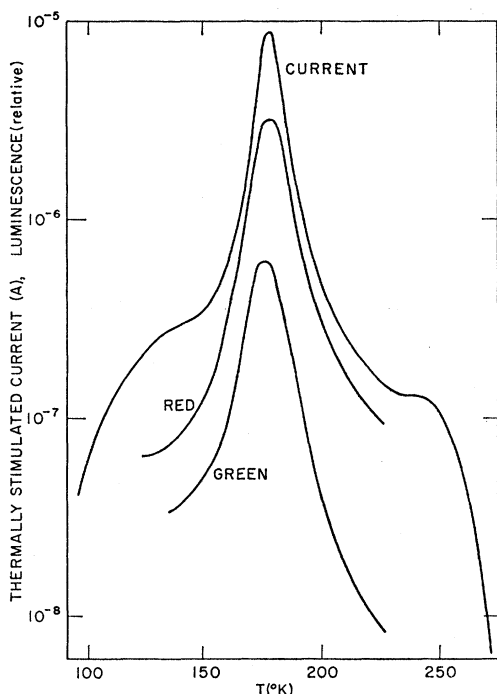


FIG. 17. Thermally stimulated current and luminescence in ZnSe:Cu:Al.

is the red luminescence emission at 1.95 eV, produced by a pair transition between a shallow level 0.012 eV below the conduction band and the ground state 0.72 eV above the valence band.⁵ I_{R2} is the red luminescence emission at 1.97 eV, produced by a transition from the conduction band to the ground state 0.72 eV above the valence band. Q_{R1} is the thermal transition with activation energy of 0.012 eV responsible for the thermal quenching of I_{R1} near 50°K.⁵ Q_{R2} is the thermal transition with activation energy of 0.72 eV responsible for the thermal quenching of the I_{R2} emission and photoconductivity; there is also an optical transition corresponding to Q_{R2} involved in optical quenching of the I_{R2} emission and photoconductivity. E_G is the excitation of green luminescence and electron photoconductivity

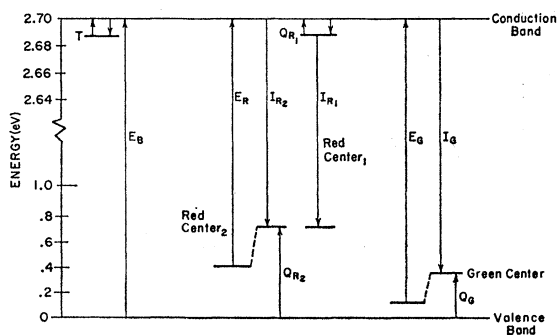


FIG. 18. Energy-level diagram for luminescence centers in ZnSe:Cu. The notation is described in the text.

with a value of 2.6 eV. I_G is the green emission at 2.34 eV. Q_G is the thermal transition with activation energy of 0.35 eV responsible for the thermal quenching of green luminescence; there is probably also an optical transition corresponding to Q_G responsible for the low-energy optical quenching of green luminescence and photoconductivity.

Evidence for Electron-Bound-Hole Luminescence Transitions

The data presented here support a model for both the red and green luminescence transitions in ZnSe:Cu, in which an electron in the conduction band, or in a shallow level below the conduction band in the case of the low-temperature 1.95-eV emission,⁵ recombines with a hole captured at a luminescence center.

The photoconductivity is n type for the excitation transitions E_R and E_G . The Hall mobility is constant while scanning the spectrum from E_R to E_G and beyond.

The thermally stimulated conductivity and luminescence curves for ZnSe:Cu:Al are identical. The free carriers responsible for the current must be the same as those involved in both luminescence transitions. Although Hall-effect measurements were not made for the TSC of the ZnSe:Cu:Al crystal, they were made for the ZnSe(SA) crystals which showed a similar TSC distribution; the carriers involved in TSC were shown to be electrons.

The transitions responsible for quenching red and green luminescence (transitions therefore which are complementary to the luminescence emission transitions) produce free holes in the valence band, as evidenced by the fact that they excite p -type photoconductivity and quench n -type photoconductivity.

It has also been reported⁵ that the long-time decay of both red and green luminescence is identical with the long-time decay of n -type photoconductivity, all three exhibiting an exponential decay controlled by the 0.012-eV shallow traps.

Acceptor Luminescence and Sensitizing Centers in ZnSe:Cu

Three effects are found in ZnSe:Cu associated with centers located at 0.72 eV above the valence band. (1) An acceptor center associated with copper impurity is seen in conductivity and Hall-effect measurements. (2) A red (1.97-eV) emission is observed. Subtracting this energy from the band gap gives 0.73 eV for the height of the corresponding level above the valence band. This agrees with the value of the activation energy obtained from thermal and optical quenching. (3) A comparison of thermal and optical quenching of red luminescence with that of photoconductivity indicates that the energy level for the sensitizing centers is also located at about 0.72 eV above the valence band.

The acceptor center is almost certainly a copper level since ZnSe was made p type by incorporation of copper.

The red luminescence center is identified as the same copper center because the red luminescence is not observed in material without copper or in materials with other impurities. The red luminescence can be removed by annealing in liquid Zn which extracts the copper.

The sensitizing center for *n*-type photoconductivity in *p*-type ZnSe:Cu is also identified as this same copper center. There are at least three reasons for this assignment. (1) The sensitizing center concentration can be estimated from the measured lifetime and electron-capture cross section to be 10^{17} cm^{-3} , which agrees well with the spectrographically determined copper concentration. (2) No transient increase in red luminescence during the optical quenching of photoconductivity and luminescence is found, as often characterizes results when luminescence and sensitizing centers are different as in *n*-type ZnS:Cu.¹⁷ (3) The alternative identification of the sensitizing center would be with an intrinsic defect, and the following section summarizes the fact that the native defect sensitizing center observed in ZnSe(SA) has quite different properties from the sensitizing center found in *p*-type ZnSe:Cu.

Sensitizing Center in ZnSe(SA)

From the measured lifetime and capture cross section of sensitizing centers in ZnSe(SA), the density of these centers is estimated to be about $5 \times 10^{17} \text{ cm}^{-3}$. Spectrographic analysis indicates no detectable impurities with concentrations greater than 10^{16} cm^{-3} . It appears likely therefore that the sensitizing centers in ZnSe(SA) are intrinsic defects. Such a conclusion is consistent with the results of Kang *et al.*¹⁷ in *n*-type ZnS:Cu:Cl; the "red" center (green in ZnS) and the intrinsic sensitizing center were both present in the same sample and at almost, but not quite, the same position in the energy gap. It was shown that they were different centers by observing a transient increase in luminescence simultaneously with a decrease of photoconductivity during optical quenching, and by observing different thermal quenching behavior for luminescence and photoconductivity.

The properties of the sensitizing center in ZnSe(SA) are different from those of the sensitizing center associated with copper in ZnSe:Cu. The level (or levels) associated with the sensitizing center in ZnSe(SA) lie closer to the valence band (0.5–0.6 eV) than the copper sensitizing center. Sensitizing centers were also slightly shallower than copper in *n*-type ZnS:Cu:Cl.¹⁷ The electron-capture cross section of the sensitizing centers in ZnSe(SA) is $3 \times 10^{-22} \text{ cm}^2$, whereas the cross section of the copper sensitizing centers is $4 \times 10^{-19} \text{ cm}^2$.

It may therefore be concluded that although copper may act as a sensitizing center under the proper circumstances, it is by no means either the only or the most

efficient sensitizing center in II-VI compounds. The identification of the sensitizing center found in *n*-type II-VI compounds with an intrinsic defect still seems necessary.

Analysis of Copper Centers

The copper centers responsible for the red and green luminescence emission may be more specifically identified as two charge states of copper impurity substituting for Zn on the ZnSe lattice. In this identification, Cu_{Zn}' is responsible for the red luminescence and is located 0.72 eV above the valence band, and Cu_{Zn}^x is responsible for the green luminescence and is located 0.35 eV above the valence band.

As summarized in the Introduction, the *d* orbitals of Cu_{Zn}^x with the $(\text{Ar})3d^9$ electronic configuration are split into *t* and *e* levels by the tetrahedral crystal field. Consideration of the selection rules for optical transitions shows that transitions from level *e* to level *t* are allowed by all rules. The magnitude of the splitting cannot be predicted from crystal-field theory, but Baranowski *et al.*² have correlated the crystal-field splitting parameter for different *dⁿ* levels in various II-VI and III-V compounds. From this work it is predicted that the crystal-field splitting should be about 0.95 eV for copper in ZnSe. According to Allen¹⁸ the actual position of Cu_{Zn}^x in the bandgap can be estimated by a correlation of the energy levels of various transition metals in the bandgap of ZnS. He estimates Cu_{Zn}^x in ZnS to be at roughly 0.6 eV from the valence band, and Cu_{Zn}' to be slightly higher. This is in rough consistency with 0.35 eV for Cu_{Zn}^x and 0.72 eV for Cu_{Zn}' in the smaller bandgap of ZnSe. Sufficient experimental information about ZnSe is not available to permit use of Birman's³ more fundamental analysis.

The bandgap diagram for the system ZnSe:Cu showing Cu_{Zn}' and Cu_{Zn}^x centers is given in Fig. 19.

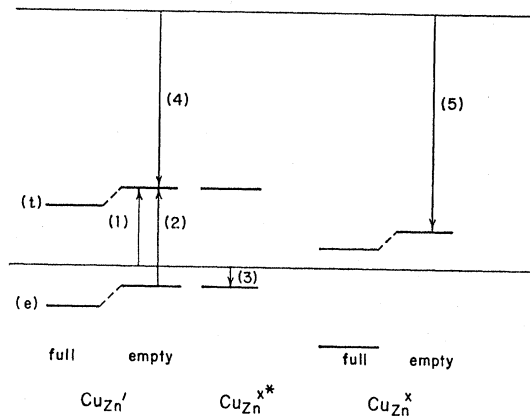


FIG. 19. Band diagram showing schematically Cu_{Zn}' and Cu_{Zn}^x centers in ZnSe:Cu.

¹⁷ C. S. Kang, P. B. P. Phipps, and R. H. Bube, Phys. Rev. 156, 998 (1967).

¹⁸ J. W. Allen, in *Proceedings of the International Conference on Semiconductors, Paris, 1964* (Dunod Cie., Paris, 1964).

With this model it is possible to interpret in detail the experimental information discussed in this paper. The following transitions are shown.

- (1) $\text{Cu}_{\text{Zn}}^{\times} + 0.72 \text{ eV} = \text{Cu}_{\text{Zn}}' + h\cdot$,
- (2) $\text{Cu}_{\text{Zn}}^{\times} + 0.93 \text{ eV} = \text{Cu}_{\text{Zn}}^{\times*}$,
- (3) $\text{Cu}_{\text{Zn}}^{\times*} = \text{Cu}_{\text{Zn}}' + h\cdot$,
- (4) $\text{Cu}_{\text{Zn}}^{\times} + e' = \text{Cu}_{\text{Zn}}' + 1.97 \text{ eV}$,
- (5) $\text{Cu}_{\text{Zn}}\cdot + e' = \text{Cu}_{\text{Zn}}^{\times} + 2.34 \text{ eV}$.

The diagram of Fig. 19 is in a sense schematic, because transitions within the $3d^9$ electronic shell, as well as between the bands and the $3d^9$ electrons, are represented in the same diagram. The center Cu_{Zn}' has an electronic structure of $(\text{Ar})3d^{10}$, and this ion is surrounded by the crystal lattice. It is possible to excite an electron from the ion to the conduction band of the crystal. The lattice relaxes because of the change of ionization state of the ion. When the electron makes the reverse transition from the conduction band to the $3d$ shell, transition (4), the energy released is less than the energy required to excite it to the conduction band (Stokes shift). An equivalent transition, as far as the state of the ion is concerned, is from the valence band to the $3d$ shell, transition (1) instead of (4); the final state is the same. Transition (2) however, does not result in the same final state. It is a transition within the $3d^9$ shell that does not change the ionization state of the ion. Transition (3), which can take place when the $\text{Cu}_{\text{Zn}}^{\times}$ is in the excited state $\text{Cu}_{\text{Zn}}^{\times*}$, is equivalent to transition (2) when the center is in the ground state. After an electron has been removed from $(\text{Ar})3d^{10}$, a second electron can be removed to give $(\text{Ar})3d^8$. The energy required to remove this second electron is naturally greater than that required to remove the first. The reverse transition, (5), results in a photon of slightly lower energy than that required to excite the electron to the conduction band. A number of internal transitions can occur within the $3d^8$ ion similar to transition (2) in the $3d^9$ ion; these are not shown in Fig. 19.

The following areas of experimental evidence may be presented in support of this detailed interpretation of the role of copper in photoelectronic effects in ZnSe.

Absorption, Optical Quenching, and Excitation of p -Type Photoconductivity

Since the position of the Fermi level at thermal equilibrium in the grown ZnSe:Cu crystals is slightly below the acceptor level, most of the copper is in the $\text{Cu}_{\text{Zn}}^{\times}$ state, with some in the Cu_{Zn}' state, and almost none in the $\text{Cu}_{\text{Zn}}\cdot$ state. Transitions (1) and (2) should therefore be seen in optical absorption. The relevant data are shown in Figs. 5 and 9. Transition (1) produces an absorption edge at 0.72 eV with the direct creation of free holes to take part in p -type photocon-

ductivity or optical quenching of n -type photoconductivity. Transition (2) is a localized transition which produces an absorption band with maximum at 0.93 eV, which produces free holes only if the hole makes a transition to the valence band via transition (3) before the excited $\text{Cu}_{\text{Zn}}^{\times*}$ center relaxes back to the ground state. The efficiency of process (2) in terms of free holes created per photon absorbed might well be appreciably smaller than process (1), resulting in a relatively larger contribution of process (1) in excitation of p -type photoconductivity or in quenching of n -type photoconductivity with respect to process (2) than in absorption. The difference between hole excitation and absorption shown in Figs. 5 and 9 is consistent with this conclusion.

The proposed model also explains why the infrared absorption disappears when the Fermi level is raised higher than 0.72 eV above the valence band by the incorporation of donor impurities into ZnSe:Cu. Raising the Fermi level above 0.72 eV from the valence band converts all the $\text{Cu}_{\text{Zn}}^{\times}$ centers to Cu_{Zn}' centers, so that transitions (1) and (2) can no longer occur.

Copper Luminescence in II-VI Compounds

According to Lehman,¹⁹ the energy-level positions of the two characteristic copper luminescence centers (red and green in ZnSe:Cu) are only slightly perturbed by the particular anions and cations surrounding the copper. These results suggest that for both centers the nature of the ion forming the center, rather than the perturbation of the lattice, is the important factor in determining the nature of the center.

p -Type Conductivity in ZnSe:Cu

It has been found^{20,21} that high-conductivity p -type ZnSe cannot be prepared by the incorporation of copper acceptors. The experimental results of the present investigation, as summarized in Table II, indicate that the Fermi level cannot be lowered below 0.54 eV from the valence band by incorporation of copper and annealing in Se to remove compensating donor Se vacancies. These results can be understood in terms of the multivalent copper impurity model. Under the conditions for maximum p -type conductivity, i.e., no compensating donors, the charge neutrality condition is $n + \text{Cu}_{\text{Zn}}' = \text{Cu}_{\text{Zn}}\cdot + p$. Given the energy levels of Cu in ZnSe, this condition reduces simply to $\text{Cu}_{\text{Zn}}' = \text{Cu}_{\text{Zn}}\cdot$, and corresponds to the Fermi level located midway between the Cu_{Zn}' level and the $\text{Cu}_{\text{Zn}}\cdot$ level, or at $\frac{1}{2}(0.72 + 0.35) \text{ eV} = 0.53 \text{ eV}$ above the valence band. Thus the model predicts that this position of the Fermi level is the lowest obtainable with the copper acceptor.

¹⁹ W. Lehman, J. Electrochem. Soc. **113**, 440 (1966).

²⁰ A. G. Fischer (private communication).

²¹ J. Dieleman (private communication).

Dependence of Dominant Copper Emission on Preparation Conditions

It is well known that, particularly in ZnS,²² the high-energy copper emission is favored by high copper concentration and low donor (coactivator) concentration, whereas the low-energy emission is favored by having the copper concentration approximately equal to or less than the donor concentration. Our results for ZnSe:Cu follow the same pattern, as shown in Fig. 16. Annealing in Se or adding additional copper to ZnSe:Cu makes the green-to-red ratio increase, whereas adding donors such as aluminum drastically decreases this ratio. Mirnov and Markovski²³ made similar observations in ZnSe, which they claimed contained no copper, but which exhibited typical copper emission.

Such results may readily be interpreted by the multivalent copper model. When the dark Fermi level is above the Cu_{Zn}' centers level, nearly all of the copper is in the Cu_{Zn}' state. There are no $\text{Cu}_{\text{Zn}}^{\times}$ centers available for green luminescence unless a Cu_{Zn}' captures two holes sequentially before capturing an electron. Therefore, when the dark Fermi level is above the Cu_{Zn}' level, red luminescence predominates. As the Fermi level is lowered, the ratio of green-to-red luminescence increases, as more $\text{Cu}_{\text{Zn}}^{\times}$ centers are available in the dark to capture photoexcited holes to become Cu_{Zn} green-emitting centers. Such a dependence of green-to-red emission ratio on the location of the dark Fermi level is found only if the concentrations of red and green centers are not electronically independent. If the concentrations of red and green centers are independent of the location of the dark Fermi level, it may easily be shown that no such variation of green-to-red ratio with Fermi level positions will be found.

Other Interpretations for High-Energy Cu Center in ZnS

Other types of measurements have led other investigators to different interpretations of the high-energy Cu center in ZnS, which should be included here for completeness. Shionoya²⁴ has observed a small polarization of the high-energy copper emission in cubic ZnS when the crystal was excited with polarized radiation, suggesting that the center has a lower symmetry than the tetragonal symmetry of a substitutional or interstitial site.

On the basis of EPR results on the high-energy Cu center in ZnS, Morigaki²⁵ identifies the center as an interstitial Cu, acting as a donor. It would be possible

²² W. Van Gool, Philips Res. Rept., Suppl. No. 3 (1961).

²³ I. A. Mirnov and L. Y. Markovski, *Fiz. Tverd. Tela* **6**, 1779 (1965) [English transl.: *Soviet Phys.—Solid State* **6**, 1779 (1965)].

²⁴ S. Shionoya, paper presented at International Conference on Luminescence, Budapest, 1966 (unpublished).

²⁵ K. Morigaki, in *II-VI Semiconducting Compounds*, edited by D. G. Thomas (W. A. Benjamin, Inc., New York, 1967), p. 1348.

to explain many of the results of this investigation by associating the green-emitting center with an interstitial Cu_i' donor; the dependence of green-to-red emission intensity on dark Fermi level position, however, does not appear consistent with a model involving electronically independent concentrations for the red and green centers. Further correlation of polarization and EPR studies with photoelectronic properties is required before these other interpretations can be fully evaluated.

CONCLUSIONS

The photoelectronic properties of ZnSe:Cu can consistently be described by a model of copper impurity substituting on the Zn sublattice. The copper is considered in terms of an ionic crystal-field description, in which the copper, perturbed by the crystal field of the lattice, is the defect which is electronically and optically active in three charge states, Cu_{Zn}' , $\text{Cu}_{\text{Zn}}^{\times}$ and Cu_{Zn} . On the basis of this model the following assignments may be made.

(1) Cu_{Zn}' is the dominant acceptor center controlling p -type conductivity in ZnSe:Cu, with energy level 0.72 eV above the valence band.

(2) Cu_{Zn}' is the major sensitizing center for n -type photoconductivity in p -type ZnSe:Cu, with an electron-capture cross section of about 4×10^{-19} cm².

(3) Red emission associated with copper impurity results from the recombination of an electron, either in a shallow level 0.012 eV below the conduction band,⁵ or in the conduction band itself, with a hole captured at the Cu_{Zn}' center.

(4) Green emission associated with copper impurity in ZnSe:Cu results from the recombination of an electron in the conduction band with a hole captured at a $\text{Cu}_{\text{Zn}}^{\times}$ center, located 0.35 eV above the valence band.

(5) The location of the dark Fermi level in ZnSe:Cu is controlled by the self-compensating activity of copper impurity. The neutrality condition that $\text{Cu}_{\text{Zn}}' = \text{Cu}_{\text{Zn}}$ fixes the lowest position of the Fermi level obtainable at 0.53 eV above the valence band.

In addition, the photoelectronic properties of ZnSe(SA) indicate that the sensitizing center for n -type photoconductivity in n -type ZnSe(SA) is an intrinsic defect, with level lying 0.5–0.6 eV above the valence band, and with an electron capture cross section of 3×10^{-22} cm².

ACKNOWLEDGMENTS

The authors express their appreciation for the variety of help received from Professor David Stevenson, Professor William Spicer, Dr. Robert Burmeister, Dr. Richard Reynolds, Dr. Paul Borsenberger, Ted Larsen, and Arthur Robinson.